Cytotoxic studies of PEG functionalized ZnO Nanoparticles on MCF-7 cancer cells

Carla Rodriguez Martinez*, Prachi Joshi**, Jose L.Vera***, Jaime E. Ramirez-Vick****, Oscar Perales**** and Surinder P. Singh****

* Department of Chemical Engineering, University of Puerto Rico Mayaguez-00680, USA, carla.rodriguez6@upr.edu
** National Physical Laboratory, New Delhi-110012, India, joship@mail.nplindia.org
***Department of Chemistry, University of Puerto Rico Mayaguez-00680, USA, jlvera@yahoo.com
**** Department of Engineering Science & Materials, University of Puerto Rico Mayaguez-00680, USA, jaimee.ramirez@upr.edu, operalesperez@yahoo.com, surinder.singh@upr.edu

ABSTRACT

We have synthesized the polyethylene glycol (PEG) functionalized zinc oxide nanoparticles (ZnONPs) and studied their cytotoxic effect on MCF-7 breast cancer cells using the MTT cell viability assay. Stable suspensions of ZnONP were produced in ethanol at room-temperature. The nanoparticles were then functionalized by mixing with an aqueous solution of PEG (MW = 8,000) under constant stirring for 24hrs. The solution was then centrifuged and lyophilized for characterization. X-ray diffraction characterization suggests the formation of wurtzite structure of ZnO. UV-visible and photoluminescence measurements exhibit the characteristic optical properties of ZnO and indicate the formation of ZnO nanoparticles. FTIR studies indicate the functionalization of the ZnO nanoparticle surface with PEG. The cell viability assay suggests the higher cytotoxicity for bare ZnO compared to PEG-ZnO nanoparticles. Further enhancement in the toxicity with UV illumination indicate the possibility to use these particles for photodynamic therapy.

Keywords: ZnO, PEG, Cytotoxicity, MCF-7

1 INTRODUCTION

Zinc oxide (ZnO), a wide band gap (3.2 eV) semiconductor is well known for its wide range of applications[1-2]. ZnO nanoparticles (ZnONPs) are believed to be non toxic, biocompatible, and have been used in products of daily use, such as sunscreen lotions and food additives. Reduction in size of ZnO to the nanoscale adds special features to the resulting structures, which include reactive oxygen species generation (ROS) [3] and strong protein adsorption [4] which can be explored for controlling cytotoxicity and other signaling events or cellular responses. Recently, Zhou, et al., assessed the solubility of ZnO wires in biofluids [5] and found the half-life of them to be in the order of a few hours, eventually dissolving into ions to be used by metabolic processes. ZnONPs have been used for killing cancer cells and activating human T cells due to their cytotoxic capacity [6]. In vitro measurements demonstrated that ZnO show preferential cytotoxicity towards cancer cells. The selectivity towards cancer cells is considered to be their inherent ability which may be optimized through size and surface engineering of ZnONPs [7]. The observed difference in cytotoxic response towards cancer cells and their counterparts suggests nanostructured ZnO as an alternative to current therapies. These have also being shown to be immunomodulators which induce the expression of immunoregulatory cytokines by normal cells leading to an alternative treatment modality [8]. Photodynamic therapy (PDT) is an established approach for the management of both early and advanced tumors as well as for conditions in the cardiovascular, endodontic and ophthalmic systems [9-10]. A key factor in PDT is the ability to produce ROS such as free radical ions such as OH^-, H_2O_2, superoxides, and singlet oxygen. The antibacterial activity and catalytic behavior of ZnO is due to its ROS production capability [11]. Li, et al., have shown that ZnO NPs in combination with existing chemotherapeutic drugs such as daunorubicin could be used for PDT and other clinical biomedical applications [12].

In our preliminary study we studied the interaction of bare and polyethyleneglycol (PEG) functionalized ZnONPs with MCF-7 breast cancer cells with and without UV radiation to assess their capability to use in PDT.

2 EXPERIMENTAL

2.1 Materials

Zinc acetate dihydrate $Zn(OOCCH_3)_2{\cdot}2H_2O$, lithium hydroxide monohydrate $LiOH{\cdot}H_2O$, Polyethylene Glycol (MW=8,000), Triton X100, 2-propanol were of reagent grade and used without further purification. Absolute ethanol and n-Hexane used were of chemical grade. 3-(4,5-Dimethylthiazol-2-yl)-2,5-diphenyltetrazolium bromide

(MTT) used was of bioreagent grade (all from Sigma-Aldrich, St. Louis, MO).

2.2 Synthesis of ZnO NPs

ZnONPs were synthesized exploiting dehydration property of alcohol at room temperature following the slightly modified method of Sphanel and Anderson [13]. 2.195g zinc acetate dihydrate was dissolved in 75 ml of ethanol at 80ºC and refluxed for 20 minutes to obtain clear solution and allowed to cool to room temperature. 0.5873g of lithium hydroxide monohydrate ($LiOH•H_2O$) was dissolved in 50 ml of ethanol using ultrasonication. The ethanolic solution of LiOH was added to metal ion solution under vigorous stirring ansd was allowed to age for 40 min. ZnO NPs powder was recovered by successive precipitation using n-hexane and centrifugation. The obtained nanoparticles were dried at 60ºC in oven.

2.3 PEG functionalization of ZnO NPs

The as-synthesized ZnONPs were encapsulated by PEG using a modified procedure of Liufu et al. [14]. 0.6069 g of ZnONPs were suspended in 40 mL of diH_2O and sonicated for 25 minutes. The solution was then brought to a pH of 8.5 with the addition of NaOH solution and sonicated again for 10 minutes. Further, a stock solution of PEG was prepared by dissolving an amount of 750 mg of PEG into 100 mL of double distilled water, and 4 mL of this solution was added to the ZnONPs solution. The reaction mixture was kept for 24 hours stirring to obtain efficient PEG adsorption. After this, the PEG encapsulated ZnONPs were washed with water and freez dried overnight.

2.4 MCF-7 cell culture and Cytotoxic Studies

MCF7 cells (ATCC, Manassas, VA,USA) were all adapted and maintained in 90% MEM supplemented with 2mM L-glutamine, 1mM sodium pyruvate, 0.01 mg/ml bovine insulin and 10% Fetal Bovine Serum (FBS) (all from Sigma-Aldrich, St. Louis, MO) and the antibiotics penicillin G (100 U/ml) and streptomycin sulfate (100 µg/ml) (Lonza, Walkersville, MD) and incubated in a humidified 5% CO_2 atmosphere at 37°C.

The effect of PEG functionalization on ZnONP cytotoxicity on MCF-7 breast cancer cells was assessed via a modified MTT assay. Growing cells were seeded at 104 cells per well in two 96-well plates containing 200 µL of complete growth medium, and allowed to recover overnight. Various concentrations of bare and PEG-functionalized ZnONPs (0.01-0.1 M) dissolved in medium were added to the wells (eight per concentration). The effect of UV irradiation on ZnONP cytotoxicity was assessed by exposing one of the two plates to UV (λ=365nm) for 4 minutes in a transilluminator (UVP BioImaging Systems). All the cells were incubated for an additional 24hrs. Cell viability and ZnONP cytotoxicity was then determined using a modification of the MTT assay [14] in which 10% Triton in isopropanol was used as a solvent for the MTT formazan crystals [15] as described elsewere [16].

2.5 Characterization

The structure of synthesized ZnO NPs was determined by X-ray diffraction (XRD) using a SIEMENS D500 unit with a Cu-Kα radiation. The average crstallite size was estimated by using tranmission electron microscope (TEM) recorded on JEM-2010 at 200 kV voltage. The Optical absorbance and photoluminescence (PL) properties of ZnO NPs were studied using a UV-vis DU 800 spectrophotometer and Fluoromax2 Photo spectrometer, respectively. The PEG functionalization of ZnO NPs was verified using FTIR measurement.

3 RESULTS AND DISCUSSION

XRD analysis of as-synthesized ZnO powders confirmed the development of hexagonal wurzite phases (Figure 1) when compared with JCPDS:36-1451 for ZnO. The XRD of ZnO NPs is plotted together with the XRD of bulk ZnO. It is being found that all peaks of ZnO NPs coincide with bulk ZnO peaks, however they are lower in intensity. Additionally, the signature peaks of NPs are not very sharp and show significant broadening attributed to their nanoscale size. As a result, the (002) peak appears to get merged with (101) peak. The particle size of ZnO NPs was confirmed by TEM micrographs shown in Figure 2. The average size of ZnO NPs is found to be in 8-9 nm range.

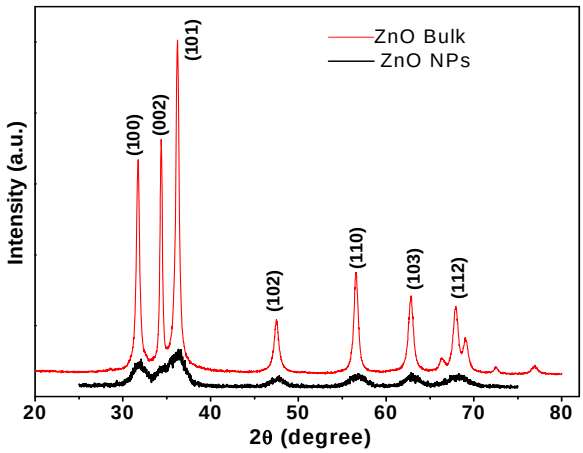

Figure 1. The representative XRD spectra of ZnO NPs in comparison with bulk ZnO.

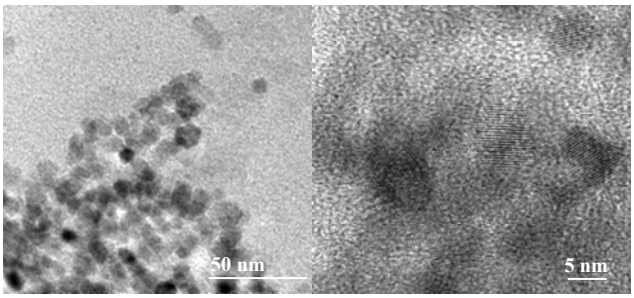

Figure 2. The TEM micrgraphs of prepared ZnONPs.

The presence of PEG at the surface of ZnO was confirmed by FTIR (Figure 3). In ZnO NPs sample, the FTIR spectrum shows the Zn-O peak at 526 cm^{-1} suggesting formation of ZnO. The peaks at 1586 and 1395 cm^{-1} are due to symmetric and asymmetric stretching vibration of C=O group of acetate suggesting presence of acetate anionic moieties at ZnO surface. The peak at 1326 cm^{-1} is assigned to symmetric C-H bending of –CH3 group of acetate and the weak broad peak around 3385 is due to O-H stretching vibration. In the FTIR spectrum of ZnO-PEG the strong peaks corresponding to carbonyl acetate are absent. The spectra of ZnO-PEG NPs shows metal oxide (Zn-O) peak at 535 cm^{-1}. The broad strong peak in 3200-3500 cm^{-1} is attributed to the absorption O-H group consisting of free O-H stretch together with hydrogen bonded O-H in ZnO-PEG NPs. The symmetric and asymmetric C─H stretching modes of ─CH_2 group are also overlapped with the broad peak of O-H group. The weak and relatively broad peak around 1376 cm^{-1} is due to C-O-H bending vibration and the peaks in 1100-1250 cm^{-1} region are attributed to C-O stretch coupled with C-C stretching vibration. The peak at 675 cm^{-1} is attributed to the long polymeric chain bending. However, the peaks in 1450-1650 cm^{-1} range suggest the presence of some acetate moieties there at the surface.

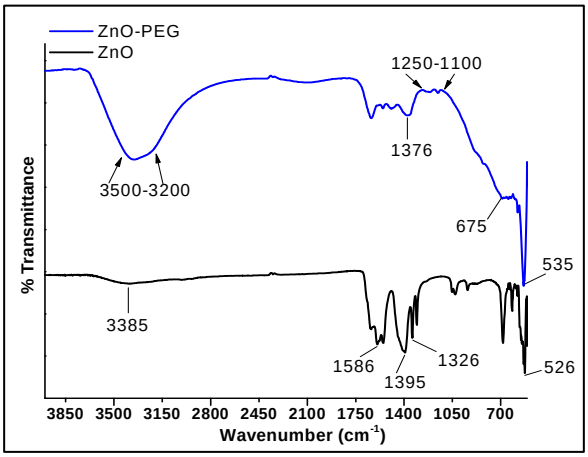

Figure 3. The FTIR spectra ZnO and ZnO-PEG NPs.

The UV-vis absorption spectra of ZnO NPs exhibit broad absorption centered around 343 nm in Figure 4. The corresponding Tauc plot (not shown) shows the band gap energy 3.39eV. The absorption of ZnO-PEG NPs is centred around 347 nm with a band gap of 3.35eV. The higher band gap energy compared to bulk is attributed to the quantum confinement effect in nano size ZnO particles. The presence of PEG at ZnO surafce reduced the absorption intensity with slight red shift in absorption $\lambda_{max.}$ The PL measurements also corroborate the formation of ZnO NPs as evidenced from the intense defect-related visible luminescence centerd around 520 nm (Figure 3) under the excitation wavelength of 330 nm. This green emission is uniquely shown by ZnO NPs that remain absent in bulk ZnO attributed to the surface defects including oxygen vacancies in nano ZnO The PEG coated ZnO NPs show red shifted defect-related emmision peak with reduced intensity at 535 nm suggesting surface passivation of ZnO NPs by PEG molecules in agreement with the UV-Vis absorption measurements.

The effect of PEG-functionalizion on ZnONPs cytotoxicity on breast cancer MCF-7 cell line were measured using a modified MTT assay at 24 hours [16]. Figures 5 and 6 show a decrease in MCF-7 cell viability with increasing time and ZnONP concentration. Table 1 present the percent increase in cell viability with PEG functionalization of the ZnONRs. Upon analysis of Table 1, it can be noted that in all cases PEG functionalization increases cell viability. The increase in cell viability could be related to the the surface passivation of ZnO nanoparticles which modulates Zn^{++} and ROS production and thus interferring the possible pathways of cytotoxicity. This is more evident in the case where the ZnONPs were exposed to UV irradiation where we could see the enhanced cytotoxic effect compare to without UV irradiation.

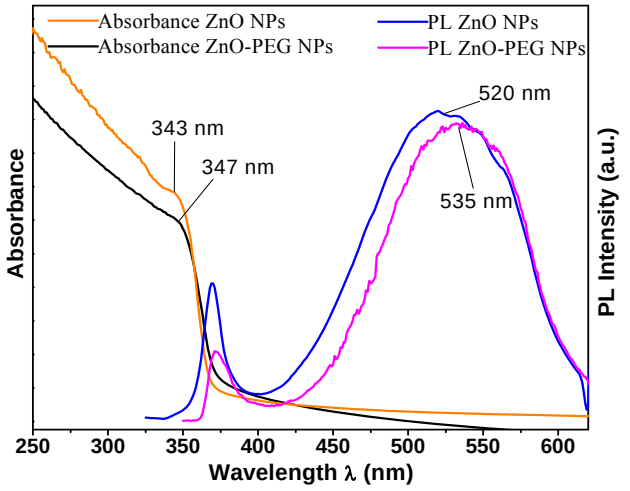

Figure 4. The optical absorption and photoluminescence (PL) spectra of ZnO and ZnO-PEG NPs.

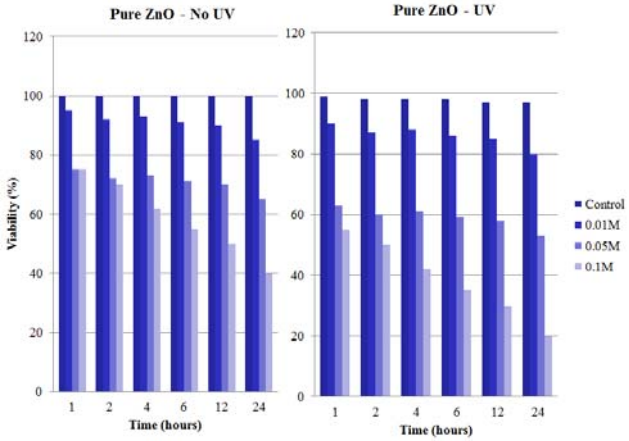

Figure 5. The effect of UV on ZnONP cytotoxicity towards MCF-7 cells a various nanoparticle concentration.

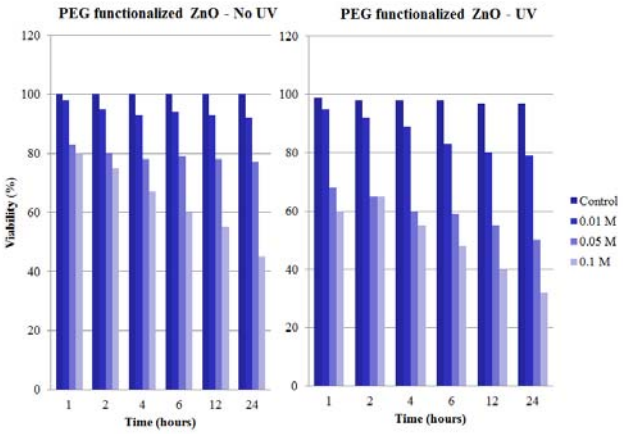

Figure 6. The effect of UV on PEG-modified ZnONP cytotoxicity towards MCF-7 cells a various nanoparticle concentration.

Table 1. Comparative increase in cell viability with PEG modification

No UV				UV			
0.0 M	0.01 M	0.05 M	0.1M	0.0 M	0.01 M	0.05 M	0.1M
0%	3%	11%	7%	0%	6%	8%	9%
0%	3%	11%	7%	0%	6%	8%	30%
0%	0%	7%	8%	0%	1%	2%	31%
0%	3%	11%	9%	0%	3%	0%	37%
0%	3%	11%	10%	0%	6%	5%	33%
0%	8%	18%	13%	0%	1%	6%	60%

4 SUMMARY

We have successfully synthesized the ZnO and PEG functionalized ZnO nanoparticles using wet chemical route and demonstrated their use as potential material system for PDT. It could be clearly seen that the PEG functionalized nanoparticles exhibit surface passivation effect in terms of reduced cytotoxicity. The concentration dependent variability in cell viability suggest a need for detailed study to optimize the optimum therapeutic concentration and specificity for different cells. The enhancement in cytotoxicity under UV irradiation suggests the potential of ZnO nanoparticles for photodynamic therapy of cancer. Detailed studies are continuing and will be published elswhere.

Acknowledgments:

NSF grants No. HRD 0833112 (CREST program) and IFN startup grant No. OIA-0701525,and NIH grant No. 1SC2GM089642, are gratefully acknowledged. JLV acknowledge the RISE-2-BEST NIH: Enhancing Biomedical Science and Biomedical Engineering in science and Technology IR25GM088023-01A1.

REFERENCES

[1] S. P Singh,.; S. K. Arya, P. Pandey, B. D Malhotra, S. Saha, K. Sreenivas, V. Gupta, Appl. Phys. Lett., 91, 063901, 2007.

[2] A. S. Kumar, M. S. Chen, Anal. Lett., 41, 141–158, 2008.

[3] W. Lin, Y. Xu, C.C., J. Huang Nanopart. Res., 11, 25-39, 2009.

[4] M. Horie, K. Nishio, K. Fujita, S. Endoh, A. Miyauchi, Y. Saito, H. Iwahashi, K. Yamamoto, H. Murayama, H. Nakano, N. Nanashima, E. Niki, and Y. Yoshida, Chem Res Toxicol, 22, 543-53, 2009.

[5] J. Zhou, N. Xu, and ZL. Wang, Adv. Materials, 18, 2432-2435, 2006.

[6] C. Hanley, J. Lyne, A. Punnoose, K. M. Reddy, I. Coombs, A. Coombs, K. Feris and D. Wingett, Nanotechnology, 19, 295103, 2008.

[7] H. Wang, D. Wingett, MH. Engelhard, J Mater Sci Mater Med., 20, 11-22, 2009.

[8] C. Hanley, A. Thurber , C. Hanna, A. Punnoose, J. Zhang , D. G. Wingett, Nanoscale Res. Lett., 4, 1409–1420, 2009.

[9] D. E. J. G. J. Dolmans, D. Fukumura, R. K. Jain, Nature Rev. Cancer, 3, 380-387, 2003.

[10] T. C. Pagonis, J. Chen, C. R. Fontana, H. Devalapally, K. Ruggiero, X. Song, F. Foschi, J. Dunham, Z. Skobe, H. Yamazaki, R. Kent, A. C. Tanner, M. M. Amiji, N. S. Soukos, J. Endod., 36, 322-8, 2010.

[11] P. Joshi, S. Chakraborti, P. Chakrbarti, D. Haranath, V. Shanker, Z.A. Ansari, S. P. Singh, V. J. Gupta, Nanosci. Nanotechnol., 9, 6427–6433, 2009.

[12] J. Li, D. Guo, X. Wang, H. Wang, H. Jiang, and B. Chen, Nanoscale Res. Lett., 5, 1063–1071, 2010.

[13] L. Sphanel, M. A. Anderson, J. Am. Chem. Soc. 113, 2826, 1991.

[14] T. Mossman, J. Immunol. Methods 65, 55-63.22, 1983.

[15] F. Denizot, R. Lang, *J. Immunol. Methods* 89, 271-277, 1986.

[16] L. M. Gao, J. L. Vera, J. Matta, E. Meléndez, J. Biol. Inorg. Chem. 15, 851-859, 2010.